ELSEVIER
SAUNDERS

Radiol Clin N Am 43 (2005) 709 – 731

RADIOLOGIC
CLINICS
of North America

Wrist MR Arthrography: How, Why, When

Luis Cerezal, MD[a,*], Faustino Abascal, MD[a], Roberto García-Valtuille, MD[a], Francisco del Piñal, MD[b]

[a]*Department of Radiology, Instituto Radiológico Cántabro, Clínica Mompía, Mompía, Cantabria 39109, Spain*
[b]*Department of Private Hand–Wrist and Plastic–Reconstructive Surgery and Hand Surgery, Mutua Montañesa, Calderón de la Barca 16-entlo, Santander 39002, Spain*

MR imaging has been used in the evaluation of a wide spectrum of joint disorders. Its multiplanar capabilities and refined tissue contrast allow detailed assessment of osseous and soft tissue pathology. MR imaging of the wrist frequently represents a diagnostic challenge for radiologists because of the complex anatomy of the wrist joint, the small size of its components, and little known pathologic conditions. MR arthrography combines the advantages of conventional MR imaging and arthrography by improving the visualization of small intra-articular abnormalities. MR arthrography of the wrist is a mildly invasive imaging technique, however, and should not be performed indiscriminately. This article reviews the current role of MR arthrography in the evaluation of wrist joint disorders taking into account the relevant aspects of anatomy, techniques, and applications.

How to perform wrist MR arthrography

Triple- (midcarpal, radiocarpal, and distal radioulnar joint [DRUJ]), double- (radiocarpal and midcarpal or radiocarpal and DRUJ), and single- (radiocarpal) compartment MR arthrography have been used in the wrist [1–11]. Intra-articular injection of a contrast agent is generally performed under fluoroscopic guidance. Sonographic, CT, or MR imaging guidance may be also used [12–14].

Multiple sites can be selected to successfully distend the midcarpal and radiocarpal joints (Fig. 1) [15]. The injection site of choice should be on the side of the patient's wrist opposite the symptoms to help distinguish iatrogenic spill into the dorsal soft tissues from a true capsular disruption. Injection sites for the midcarpal compartment include the distalmost scaphocapitate and triquetrohamate spaces [15]. Injection should continue until the contrast is readily visualized in the capitolunate joint space. In normal arthrograms, contrast flows into both the scapholunate (SL) and lunotriquetral (LT) spaces. The intrinsic ligaments at the proximal margins of the scaphoid, lunate, and triquetral bones arrest the proximal flows of contrast, preventing communication with the radiocarpal compartment. For radiocarpal joint ulnar-sided injections, the needle should be directed to the proximal edge of the triquetrum at the pisiform radial margin. For radial-sided injections, the needle should be directed to the radioscaphoid space away from the SL joint. Because of the natural volar tilt of the distal radius, a slight angulation of the imaging intensifier in the cranial direction facilitates better profiling of the radioscaphoid space. This prevents the needle-tip from striking the dorsal lip of the radius, which frequently overlays the radioscaphoid space on a true posteroanterior projection. Alternatively, the needle-tip can be directed into the proximal scaphoid at the margin of the radial styloid. Contrast generally fills the dorsal recess of the radiocarpal joint; however, care must be taken not to inject the area from the scaphoid distal to the scaphoid tubercle or inadvertent filling of the midcarpal joint may occur [15].

* Corresponding author.
E-mail address: lcerezal@mundivia.es (L. Cerezal).

0033-8389/05/$ – see front matter
doi:10.1016/j.rcl.2005.02.004

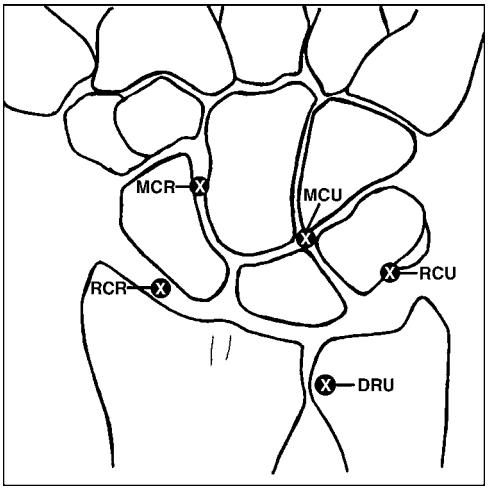

Fig. 1. Diagram illustrating the injection sites for wrist joint MR arthrography. DRU, distal radioulnar joint site; MCR, midcarpal radial site; MCU, midcarpal ulnar site; RCR, radiocarpal radial site; RCU, radiocarpal ulnar site.

The radiocarpal joint communicates with the piso-triquetral joint in 34% to 70% of patients.

The DRUJ surrounds the head of the ulna and extends to, but does not include, the ulnar aspect of the radius. Placement of the needle at the midpoint of the DRUJ space can result in an extra- as well as an intra-articular injection. The needle-tip should be directed toward the head of the ulna near its radial margin. After the needle touches the ulnar head, it should be slightly directed radially to advance deeper into the joint space thus stabilizing the needle [15]. It is important that the injected contrast show the fovea at the base of the ulnar styloid to establish where there is a defect in the ulnar attachment of the triangular fibrocartilage (TFC).

Triple-compartment wrist arthrography is performed using the following technique: first, the patient is positioned supine on the fluoroscopic table with the wrist in neutral rotation and slight volar flexion. Traction on the patient's hand is helpful, but not essential, for a successful injection. After skin preparation with a povidone–iodine solution, a 25-gauge needle is inserted under fluoroscopic guidance directly through the skin from a dorsal approach. Small-bore needles (25-gauge) used for wrist arthrography have the advantage of minimizing tissue trauma and postinjection leakage of joint fluid. The needle position is verified by a test injection of a small amount of iodinated contrast agent (approximately 1–2 mL) before administering diluted gadolinium. If the needle is intra-articular, the contrast solution flows away from the needle-tip drawing the capsular recesses. Subsequently, a solution of 0.1-mL gadolinium diluted in 20 mL of a solution composed of 10 mL of saline, 5 mL of iodinated contrast material, and 5 mL of lidocaine 1% is injected [16]. Triple-compartment MR arthrography is performed first with the injection into the midcarpal joint [17]. A total volume of 3 mL to 4 mL of solution is injected. If communication with the radiocarpal joint is present, an additional 3 mL to 4 mL of solution is injected. If communication with the radiocarpal joint and the DRUJ occurs, a further additional 1 mL to 2 mL of solution is added, for a total of 7 mL to 9 mL. If no communication is present, the radiocarpal joint and the DRUJ are sequentially injected with 3 mL to 4 mL and 1 mL to 2 mL of the solution, respectively.

Saline solution may be injected as arthrographic contrast material; however, the imaging characteristics of intra-articular gadolinium provide specific advantages over saline [12–14]. Saline within the joint is similar to a high-signal joint effusion seen on T2-weighted sequences and, although fluid collections in the vicinity of the joint are evident with T2-weighted images, it is not possible to determine whether the fluid collections are separate from the joint space or if they have occurred as a result of the saline injection.

Radiocarpal joint injection can be performed easily without imaging guidance using recognized palpable landmarks and avoiding the use of iodinated contrast medium and ionizing radiation [18]. This is especially useful in cases of limited access to a fluoroscopic suite. The injection site represents the arthroscopic 3-4 portal, an anatomic sulcus located between the extensor pollicis longus and index finger extensor digitorum communis tendon, just distal to Lister's tubercle, which provides the initial reference. The extensor pollicis longus tendon is easily palpated just ulnar to Lister's tubercle. The index finger extensor digitorum communis tendon is palpated just ulnar to the extensor pollicis longus tendons. Palpation at the 3-4 portal reveals a depression that is more defined when the patient alternatively extends the thumb (contracting the extensor pollicis longus tendon) and fingers (contracting the extensor digitorum communis tendons). With deep palpation during radiocarpal flexion and extension, the level of the dorsal lip of the radius can be estimated by feeling the mobile carpus as it moves on the fixed radius. The skin entry site is approximately 0.5 cm distal to the dorsal lip of the radius so that needle entry is angulated parallel to the distal radial articular surface (approximately 10–15°). The injection needle typically requires insertion to a depth of 0.5 cm to 1.5 cm [18]. During injection, radiocarpal distention

is usually visible and ballotable, particularly in the so-called "anatomic snuffbox" region. Although injections can be performed successfully without fluoroscopy guidance, it is advisable to have it ready available as a useful and reassuring tool when initially learning the injection procedure [18].

The current authors perform triple-compartment MR arthrography with fluoroscopic guidance in patients who have chronic pain of unclear origin or instability syndromes of the wrist. In cases of suspected TFC complex (TFCC) or intrinsic ligaments lesions, the authors prefer to practice conventional MR imaging complemented with radiocarpal MR arthrography performed directly in the MR suite, based on anatomic landmarks without fluoroscopic guidance. Only in selected cases, when suspected lesion of ulnar attachment of TFC exists at conventional MR imaging, do they perform double-compartment (radiocarpal and DRUJ) MR arthrography with fluoroscopic guidance. MR images should be obtained shortly after conventional arthrography to minimize absorption of contrast and guarantee the desired capsular distention [12–14].

MR imaging evaluation of the wrist has lagged behind that of other larger joints because of the technical limitations of spatial resolution and the signal-to-noise ratio when imaging the small structures of the wrist [19,20]. Many of the larger ligaments around the wrist are no greater than 1 mm to 2 mm thick. High-resolution MR imaging is essential in evaluating normal features and pathologic conditions of the wrist. Recent advances in MR imaging coil design have dramatically changed the capabilities of studying small hand and wrist structures. Adapted wrist coils, such as quadrature, phased array, and special microscopy coils designed for high-resolution wrist imaging, optimize spatial and contrast resolution for the small field of view (3–10 cm) and thin slice thickness (1–2 mm) [19].

Imaging in the coronal, axial, and sagittal planes should be performed in comprehensive wrist evaluation. Demonstration of the intrinsic intercarpal ligaments and TFCC are best identified with the coronal plane [21].

Numerous MR imaging sequences are currently available for wrist assessment [22]. T1-weighted spin-echo sequences with and without fat suppression maximize the signal intensity of contrast solution. Fat suppression is crucial in MR arthrography because fat and gadolinium have similar signal intensities in T1-weighted images, which makes diagnosis difficult. Fat suppression selectively decreases the signal from fat and the signal from the contrast solution is preserved, thereby confirming or excluding extra-articular contrast material. At least one fat-suppressed T2-weighted sequence should be performed for the detection of subtle bone marrow edema and extra-articular fluid collections. Three-dimensional gradient echo images are helpful in the assessment of TFCC and ligaments [23–28]. Overall, the choice of sequence depends on the preferences of the radiologist and sequence availability.

As with any invasive procedure, it is important to consider the potential risks of wrist MR arthrography [9]. The use of iodinated contrast material to confirm intra-articular needle placement carries a small risk of reaction. Slight joint pain is relatively common but usually disappears within the first few hours after puncture. Vasovagal reactions are rare and managed easily in the fluoroscopic suite so that routine administration of prophylactic atropine before arthrography is unnecessary. The most serious complication of arthrography is joint infection. Its incidence is rare. Currently, no side effects from intra-articular gadolinium solution use have been reported [9].

In terms of pitfalls, the most common are extracapsular contrast injection and extravasation of contrast material outside the joint, possibly as a result of overdistention, which can be mistaken for capsular disruption. Inadvertent use of undiluted gadolinium leads to T1 and T2 shortening and very little fluid appearing in signal. Air bubbles introduced during injection may mimic loose bodies, although generally they are in nondependent positions [12–14].

Why and when to perform wrist MR arthrography

Triangular fibrocartilage complex

In 1981, Palmer and Werner [29] introduced the term "triangular fibrocartilage complex" to describe the complex of soft tissues interposed between the distal part of the ulna and the ulnar carpus. In most descriptions the TFCC is composed of the TFC proper, the meniscus homologue, the ulnar collateral ligament (UCL), the dorsal and volar radioulnar ligaments, the subsheath of the extensor carpi ulnaris tendon or infratendinous extensor retinaculum, and the ulnocarpal ligaments (Fig. 2) [29,30]. Proximally, the TFCC originates at the ulnar aspect of the sigmoid notch of the radius extending toward the ulna pole and into the fovea at the base of the ulnar styloid. Two types of ulna attachments are observed. The most common is composed of two striated fascicles: one inserted at the base of the styloid and the other at the styloid tip. A less common insertion is

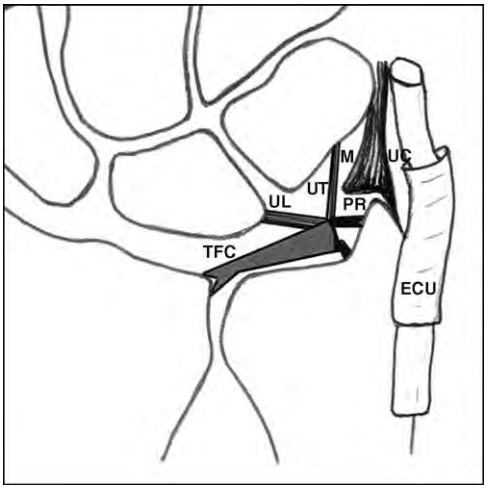

Fig. 2. Anatomy and schematic drawing of the TFCC. ECU, extensor carpi ulnaris tendon; M, meniscus homologue; PR, prestyloid recess; TFC, triangular fibrocartilage; UC, ulnar collateral ligament; UL, ulnolunate; UT, ulnotriquetral ligament.

a broad-based striated fascicle attachment along the entire length of the ulnar styloid [27]. Distally, the TFCC extends into the hamate, triquetrum, and base of the fifth metacarpal [29,30], and distally, it is joined by fibers of the UCL.

The TFC is a semicircular, fibrocartilaginous, biconcave structure interposed between the ulnar dome and the ulnar aspect of the carpus. TFC thickness is inversely proportional to the ulnar variance: ulna-minus wrists have thick TFC and vice versa. The peripheral attachment of the TFC is ~5 mm thick, thinning at the center, and then narrowing to less than 2 mm [30].

From the anterior edge of the TFC, two groups of longitudinally-oriented collagen fibers emerge: the ulnotriquetral ligament, which runs distally and into the volar aspect of the triquetrum, and the ulnolunate ligament, which runs obliquely and then distally inserted into the lunate (Fig. 3) [29,30]. The thick, strong peripheral margins of the TFC, which are composed of lamellar collagen, are often referred to as the dorsal and volar radioulnar ligaments.

The meniscus homologue is an ill-defined region of well-vascularized and loose connective tissue on the volar side of the wrist. It has a common origin with the dorsal radioulnar ligament on the dorsoulnar corner of the radius. The meniscus homologue inserts directly into the triquetrum and partially or completely separates the pisotriquetral from the radiocarpal joint [30].

The extensor carpi ulnaris tendon is located within a dorsal notch in the distal ulna. The extensor carpi ulnaris subsheath makes a significant contribution to

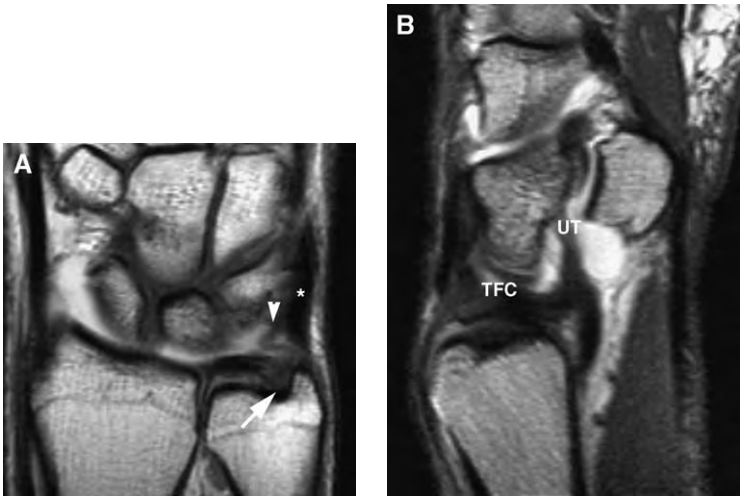

Fig. 3. Anatomy of the TFCC. (*A*) Coronal T1-weighted MR arthrogram showing a normal TFCC. The TFC appears as a low-signal intensity triangular structure. Note the striated appearance of ulnar insertion of the TFC (*arrow*). The meniscus homologue appears as an ill-defined low-signal region on the volar ulnar side of the wrist (*arrowhead*). The extensor carpi ulnaris tendon subsheath fuses with the dorsal aspect of the TFC (*asterisk*). (*B*) Sagittal T1-weighted MR arthrogram image showing the normal discoid appearance of the TFC and a longitudinally-oriented ulnotriquetral ligament, which courses distally until its insertion into the volar aspect of the triquetrum. TFC, triangular fibrocartilage; UT, ulnotriquetral ligament.

the stabilization of the dorsal TFCC because some of its fibers fuse to it [30].

The blood supply of the TFCC originates from the ulnar artery (through the radiocarpal branches) and the anterior interosseous artery (through the dorsal and volar branches). These vessels only peripheraly penetrate 10% to 40% of the TFCC, and the central and radial portions are avascular [31–33]. This pattern of supply has direct implications to the healing potential following injury of the TFC and the radioulnar ligaments, with peripheral ulnar-sided detachments demonstrating a superior healing capacity following repair when compared with radial-sided detachments.

The TFCC has three main functions. (1) it is the major stabilizer of the DRUJ and one of the stabilizers of the ulnar carpus. The primary function of radioulnar ligaments is to prevent volar and dorsal subluxation at the DRUJ. (2) The TFCC is also a load-bearing structure between the ulnar head and lunate and triquetrum. And (3) the ulnolunate and ulnotriquetral ligaments prevent volar subluxation of the ulnar carpus [29,30].

Triangular fibrocartilage complex tears

TFCC lesions may be variable in their extent of involvement. They may be confined to TFC or involve one or more components of the TFCC. Degenerative and traumatic tears of the TFC may occur. Degenerative tears are more common than traumatic tears. The incidence of central degenerative tears is age-related. According to Mikic [34], degeneration begins in the third decade and progressively increases in frequency and severity in subsequent decades. The changes are more frequent and more intense on the ulnar surface, and they are always situated in the central part of the TFC [35,36].

In 1989, Palmer [37] proposed a classification system for TFCC tears that divided these injuries into two categories: traumatic (class I) and degenerative (class II). Traumatic tears are more common in younger patients and are subclassified according to the site of TFCC involvement (Fig. 4). Class IA, the central perforation, represents a tear or perforation of the horizontal portion of the TFCC, usually occurring as a 1- to 2-mm slit, and located 2 to 3 mm medial to the radial attachment of the TFCC. Class IB represents a traumatic avulsion of the TFCC from its insertion site into the distal portion of the ulna, sometimes with an associated fracture at the base of the ulnar styloid. Class IC represents distal avulsion of the TFCC at its site of attachment to the lunate or triquetrum reflective of a tear of the ulnolunate or ulnotriquetral ligaments. A class ID lesion represents an avulsion of the TFCC from its attachment to the radius at the distal aspect of the sigmoid notch, which may be associated with an avulsion fracture of this region.

The degenerative types reflect the progressive stages of ulnar impaction syndrome and are subclassified according to the degree of involvement of structures on the ulnar side [37,38], highlighting the progressive nature of these injuries (Fig. 5). Class IIA injuries represent TFC wear from the undersurface, occurring in the central horizontal portion, without perforation. Class IIB includes TFC wear with associated lunate or chondromalacia. Class IIC injuries represent TFC perforation with lunate or ulnar

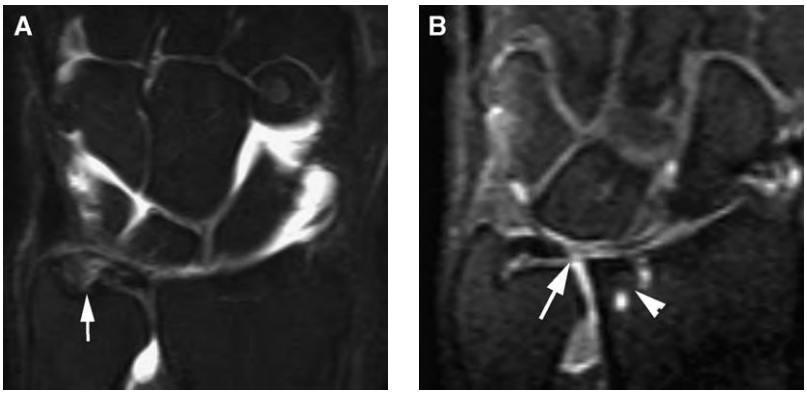

Fig. 4. Traumatic tears of the TFCC. (*A*) Coronal fat-suppressed T1-weighted radiocarpal MR arthrogram image showing traumatic avulsion of the ulnar attachment of the TFC (Palmer class IB lesion) with contrast leakage into the distal radioulnar joint (*arrow*). (*B*) Coronal fat-suppressed T1-weighted radiocarpal MR arthrogram image revealing an avulsion of the TFC from its attachment to the radius (*arrow*), associated with an avulsion fracture at the distal aspect of the sigmoid notch (*arrowhead*) (Palmer class ID lesion).

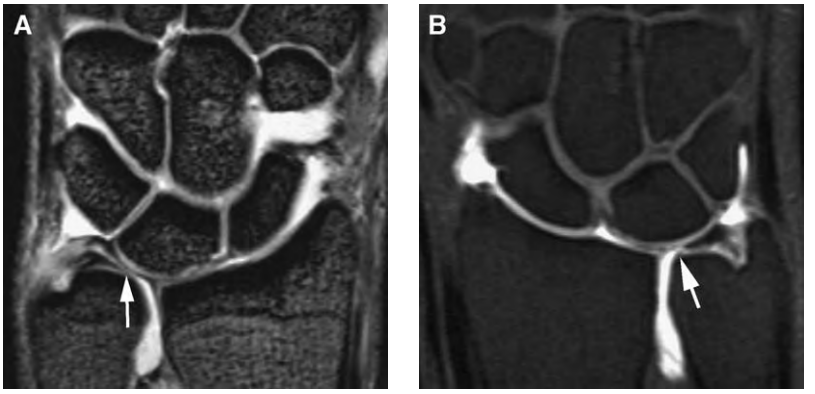

Fig. 5. Degenerative tears of the TFCC. (*A*) Palmer class IIB lesion (ulnar impaction syndrome). Coronal T2*-weighted MR arthrogram image revealing a degenerative partial tear of the proximal surface of the central portion of the TFC and thinning without perforation (*arrow*). Note the existence of positive ulnar variance. (*B*) Palmer class IIC lesion (ulnar impaction syndrome). Coronal fat-suppressed T1-weighted MR arthrogram image showing a central TFC perforation with contrast material communication between the radiocarpal and distal radioulnar compartments (*arrow*).

chondromalacia. The perforation is in the central, horizontal portion of the TFC and occurs in a more ulnar location than that seen with the traumatic injury that occurs in this region (class IA). Class IID lesions include TFC perforation in the central horizontal portion associated with lunate or ulnar chondromalacia and LT ligament perforation. Class IIE injuries include TFC perforation associated with lunate or ulnar chondromalacia, LT ligament perforation, and additional ulnocarpal arthritis.

Clinical diagnosis. Tears of the TFCC result in ulnar-sided wrist pain and tenderness often with a palpable or audible click when the forearm is rotated. Although some degenerative tears or defects may not be symptomatic [39,40], examination usually reveals point tenderness volar to the extensor carpi ulnaris tendon and just distal to the ulna. Plain radiographs may be completely normal or may be significant for positive ulnar variance with cystic changes of the ulnar aspect of the lunate consistent with ulnar impaction.

MR imaging and MR arthrography. The TFCC appears as a low-signal intensity on MR images. The TFC specifically is triangular on coronal sections with its apex attaching to the intermediate-signal intensity hyaline articular cartilage of the ulnar aspect of the sigmoid notch of the radius with separate superior and inferior bifurcate attachments [20,27]. On axial images, the TFC is shaped like an equilateral triangle with the apex converging on the ulnar styloid and the base attaching on the superior margin of the distal radial sigmoid notch. On sagittal images it appears thicker on the volar and dorsal aspects. Its ulnar attachment may appear bifurcated with two bands of lower-signal intensity attached to the fovea at the base of the radial aspect of the ulnar styloid and to the ulnar styloid itself separated by a region of higher-signal intensity [20,27]. These sites of increased signal at the ulnar attachments and at the hyaline cartilage of the sigmoid notch of the radius should not be mistaken for detachments or tears. Both the distal and proximal surfaces of the TFC are depicted on MR images; information that is not available with wrist arthroscopy.

The prestyloid recess is an extension of the radiocarpal joint, which lies near the ulnar attachment of the TFC. Fluid collected in the prestyloid recess between the TFC and meniscus homologue produces increased signal intensity on T2-weighted images. Contrast may accumulate in this region normally at MR arthrography.

In older patients a signal may be seen within the low-signal TFC on T1-weighted and proton-density–weighted MR images that is thought to be caused by mucoid and myxoid degenerative changes. Degeneration of the TFC is frequently seen and often asymptomatic [39,40]. When there is degeneration of the TFC, MR imaging shows intermediate-signal intensity on short-echo-time images that does not increase on T2- or T2*-weighted images. If such signal changes do not communicate with the inferior or superior surface of the TFC, and if the signals are not any brighter on images with T2 contrast, then the TFC degeneration is not indicative of a tear. Degenerative changes may also manifest as thinning or attenuation of the TFC. Progressive degeneration of

the proximal surface leads to erosion, thinning, and perforation of the TFC. In partial degenerative tears (Palmer classes IIA and B), the signal extends only to one articular surface. With complete tears the signal extends to proximal and distal articular surfaces. Discontinuity or fragmentation of the TFC may also be seen. Fluid collecting in the DRUJ is an important secondary sign, but the presence of fluid signal alone is not indicative of a TFC tear.

In MR imaging there are no specific differentiating features separating a traumatically-induced tear of the TFC from one caused by degeneration. The appearance of these lesions may also be similar in symptomatic and asymptomatic individuals; determining the clinical relevance of these lesions and their correlation with patients' symptoms may be difficult. Patient age, tear location, clinical history, and associated lesions are often criteria that may be needed to differentiate their origin.

Many studies have investigated the usefulness of conventional MR imaging in the detection of TFC tears [41–45]. Degenerative (Palmer class II) and traumatic radial tears of the TFC (Palmer classes IA and D) may be confidentially appreciated with MR imaging. Reported sensitivities, specificities, and accuracies compared with arthroscopy are above 90% for degenerative (Palmer class II) tears [41,44,45]. Traumatic tears of the ulnolunate or ulnotriquetral ligaments (Palmer class IC) and traumatic avulsions of the TFCC from its ulnar insertion (Palmer class IB), however, are more difficult to diagnose. MR imaging findings that correlate with ulnar-sided type of tears include altered morphology of the ulnar attachments of the TFC, excessive fluid localized to this region, and linear fluid signal in the ulnar TFC itself extending to its surface. Oneson et al [44], in an MR imaging study of TFCC tears that underwent arthroscopic evaluation, had a poor sensitivity to ulnar tears for two observers (25% and 50%, respectively). Haims et al [41] most recently confirmed the limitations of conventional MR imaging in the diagnosis of peripheral ulnar-sided tears of the TFC. They found the evaluation sensitivity of tears of the peripheral TFCC to be 17%, with a specificity of 79% and an accuracy of 64%. The poor diagnostic accuracy was attributed to the presence of normal striated fascicles at the periphery of the TFCC and fluid that collected on the ulnar aspect of the wrist [41].

Not uncommonly, fluid signal and thickening may be present along the ulnar aspect of the TFCC. This appearance may be caused by degenerative or inflammatory changes, or as a result of a prior, healed peripheral TFC injury with scarring and chronic synovitis. This type of injury may be difficult to differentiate from an acute peripheral TFC injury. Correlation with the patient's clinical history is helpful to this end [45].

Although initial experience with MR arthrography in the assessment TFCC lesions did not show sufficient benefit over conventional MR imaging [3,10], the most recent MR arthrography studies using up-to-date technology have improved sensitivity, specificity, and accuracy for the evaluation of partial and complete tears of the TFCC [1,4,8]. In a recent MR arthrography study of 125 patients who had arthroscopic correlation, Schmitt et al [8] reported sensitivity of 97.1%, specificity of 96.4%, and accuracy of 96.8% for the detection of TFCC lesions.

The principal usefulness of MR arthrography resides in the evaluation of TFC peripheral ulnar tears. MR arthrography is also helpful in the detection of partial tears of the undersurface by revealing contrast extending through and outlining the TFC defect. Injection from the DRUJ may best outline such partial-thickness tears.

Treatment. The treatment of TFCC tears is complex and ongoing. Central tears (class IA) are treated with arthroscopic debridement by enlarging the tear in such a way that the fibrocartilage flaps can no longer make contact [46,47]. If a class IA tear is associated with an ulna-plus, simple debridement of the tear is insufficient and a formal ulnar shortening or an arthroscopic resection of the dome of the ulnar head (the so-called "arthroscopic wafer" procedure) is most appropriate [48,49]. The periphery of the TFCC is penetrate by blood vessels and has the ability to heal itself [31]. This has been opportunely used to reinsert (open surgery or an arthroscopic reinsertion) the peripheral type of TFCC tears (class IB) to the capsule with good results [50]. As for class IA, correction of a concomitant ulna-plus is mandatory: repair of a tear without considerations of the ulna discrepancy leads to failure of the procedure [51,52]. In time peripheral tears may lose the ability to heal themselves and repair is no longer possible. Whether because of long delays after the injury, or because no local tissues are available, reconstruction of DRUJ stability requires tendon graft plasty techniques [53]. Avulsion of the ulnocarpal ligaments (class IC) is rarely an isolated injury, but often part of a generalized ligamentous derangement [54]. Treatment depends on the stage and can be successfully performed by open surgery or arthroscopic treatment [47]. Avulsion of the TFC from the very edge of the radius (class ID) should be differentiated from the central-most type IAs because the latter are not repairable. In class ID, however, the TFC can be

successfully reinserted into the radius and repaired with an open procedure or arthroscopic method [55].

Ligamentous anatomy

The carpal ligaments are divided into two major groups: in- and extrinsic ligaments [56]. The intrinsic, or intraosseous ligaments, are entirely within the carpus and connect the individual carpal bones. The extrinsic ligaments link the carpal bones to the radius and ulna. The description of the volar and dorsal extrinsic ligaments varies considerably [2,17,57–60], perhaps because of anatomic variation, but also that these ligaments are not discrete structures but rather focal thickenings of the fibrous capsule. The volar complex is the stronger of the two and seems to play a larger role in wrist stability. Recent anatomic studies suggest, however, that the dorsal ligaments of the wrist play an even larger and more important role in carpal stability and carpal kinematics than was previously recognized [61–63].

Volar ligaments

Volar radiocarpal ligaments. The volar extrinsic radiocarpal ligaments are comprised of the radioscaphocapitate, radiolunotriquetral or long radiolunate, radioscapholunate, and short radiolunate ligaments (Fig. 6) [2,17,56–58,60]. The radioscaphocapitate is a prominent ligament, which extends from the radial styloid through a groove in the waist of the scaphoid to the volar aspect of the capitate.

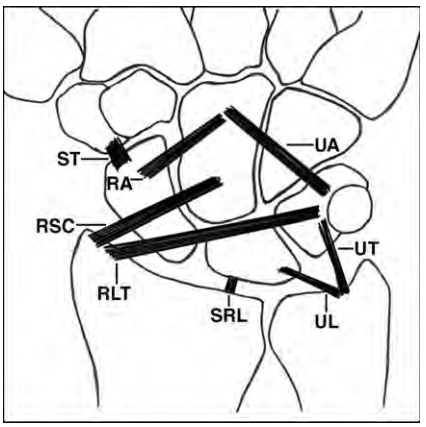

Fig. 6. Anatomy of the volar ligaments. Diagram illustrating the extrinsic radio- and ulnocarpal ligaments and intrinsic scaphotrapezial and deltoid ligaments. RA, radial arm of the deltoid ligament; RLT, radiolunotriquetral; RSC, radioscaphocapitate; SRL, short radiolunate ligaments; ST, scaphotrapezial ligament; UA, ulnar arm of the deltoid ligament; UL, ulnolunate ligament; UT, ulnotriquetral ligament.

The radiolunotriquetral ligament arises from the volar aspect of the radial styloid. The radiolunotriquetral and radioscaphocapitate ligaments share the same radial attachment site, with the radiolunotriquetral further extending to the ulnar side of the distal radial volar surface. The radiolunotriquetral ligament travels distally and ulnar-ward through the groove of the scaphoid proximal to the radioscaphocapitate ligament and widely inserts into the volar aspect of the triquetrum. The radiolunotriquetral ligament is made up of the radiolunate and LT portions. As such it has also been referred to as separate long radiolunate and volar LT ligaments [17].

The radioscapholunate ligament, or ligament of Testut, arises from the volar aspect of the distal radius at the prominence between the scaphoid and lunate fossa, and extends distally inserting itself into the proximal volar aspect of the scaphoid, lunate, and SL ligaments. The radioscapholunate ligament, previously thought to be an important scaphoid stabilizer, is now considered to be a neurovascular pedicle derived from the anterior interosseous and radial arteries and anterior interosseous (Fig. 7) [64]. The short radiolunate ligament, which is contiguous to the TFCC volar fibers, originates from the volar margin of the distal part of the radius and inserts into the proximal part of the volar surface of the lunate.

Volar ulnocarpal ligaments. The volar ulnocarpal ligaments are comprised of the ulnolunate and ulnotriquetral ligaments. They originate at the volar edge of the TFC and insert into the lunate and the triquetrum, respectively [2,17,57–60]. The arcuate, or deltoid ligament, is a V-shaped volar intrinsic ligament with a capitotriquetral (ulnar) and a capitoscaphoid (radial) arm.

Dorsal ligaments

The dorsal radiocarpal ligament, also called dorsal radiotriquetral, arises from the dorsal aspect of the distal radius and extends distally over the dorsal aspect of the lunate to insert on the dorsal aspect of the triquetrum [62,63]. The dorsal radiocarpal has been grouped into four types by Viegas et al [63] according to a modification of Mizuseki and Ikuta's [62] classification: type I, the ligamentous fibers are attached to the dorsal margin of the distal ulnar aspect of the radius, then extend to the dorsal tubercle of the triquetrum (54%); type II, the same basic pattern as in type I with an additional ligamentous branch between the dorsal tubercle of the triquetrum and the dorsal margin of the distal radius at its extensor carpi radialis level (24%); type III, in addition to the type II pattern, there are more thin fibers spanning from the

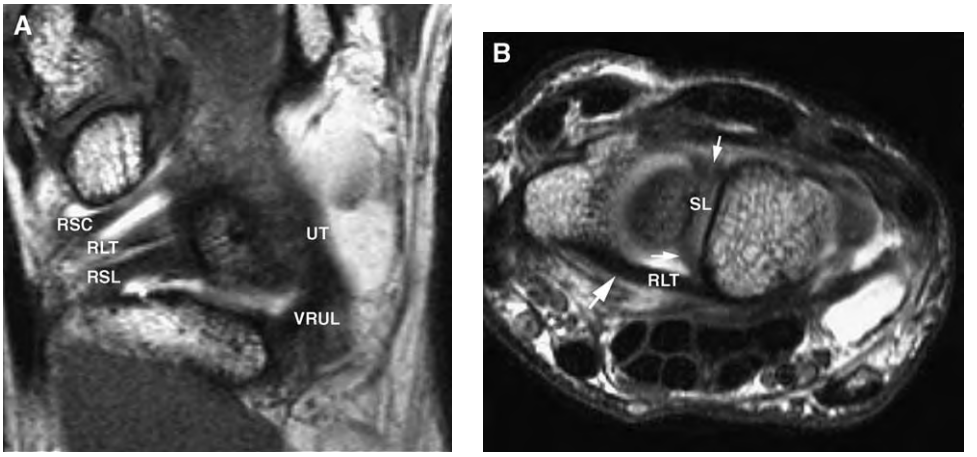

Fig. 7. Anatomy of the volar ligaments. (*A*) Coronal T1-weighted MR arthrogram image showing the radioscaphocapitate (RSC), the radiolunotriquetral (RLT), and the radioscapholunate (RSL) ligaments in the volar radial aspect of the wrist. The volar radioulnar (VRUL) and ulnotriquetral (UT) ligaments are seen in the ulnar aspect of the wrist. (*B*) Axial T1-weighted MR arthrogram image showing the thick radiolunotriquetral (RLT) ligament (*large arrow*). Note the dorsal and volar components (*small arrows*) of the scapholunate (SL) ligament.

dorsal triquetrum to the dorsal radius between the main ligament and the ligamentous branch (12%); and type IV, a type I pattern with additional separate ligamentous fibers from the ulnar aspect of the radius (9%) (Fig. 8) [63].

The dorsal intercarpal ligament originates from the dorsal tubercle of the triquetrum. It attaches to the dorsal distal aspect of the lunate and inserts into the dorsal groove of the scaphoid and dorsal proximal rim of the trapezium. The proximal side of this transversely oriented ligament is thicker than its distal side. This ligament attaches not only to the lunate and scaphoid but also to the SL ligament and the LT ligament.

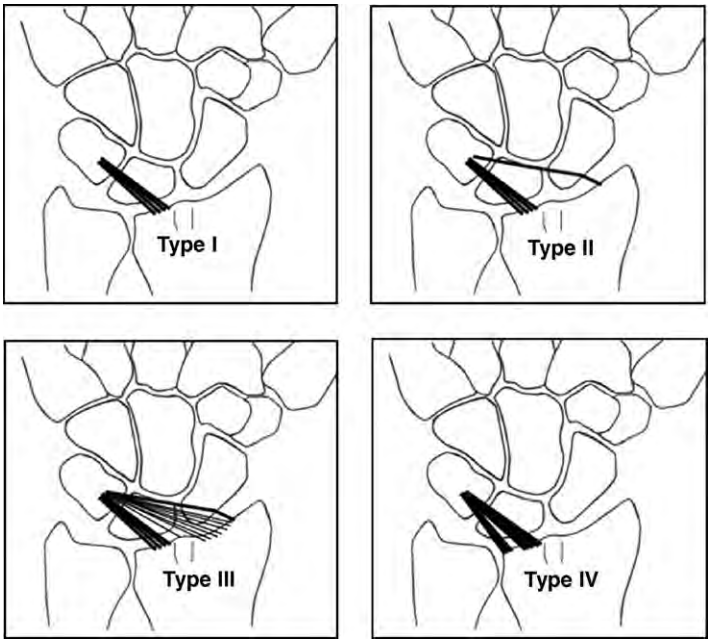

Fig. 8. Diagram illustrating the four types of dorsal radiocarpal ligaments.

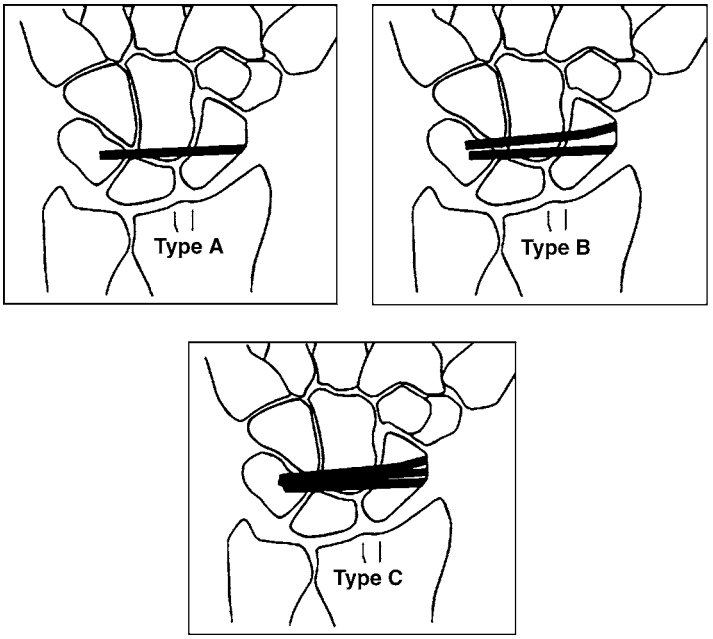

Fig. 9. Diagram illustrating the three types of dorsal intercarpal ligaments.

The dorsal intercarpal ligaments have been classified into three types: type A, a single thick fiber or net of thin fibers (30%); type B, two thick fibers (44%); and type C, three or more fibers (26%) (Fig. 9) [63].

Intrinsic ligaments

The most important intrinsic ligaments are the SL and LT ligaments (Fig. 10). These ligaments link the bones of the proximal carpal row on their proximal surfaces, separate the radio- from the midcarpal compartments, and provide flexible linkage so that the proximal carpal row functions properly. These ligaments have three components: (1) dorsal, (2) proximal, and (3) volar. Although the dorsal and volar components mostly consist of collagen fibers, the proximal, or membranous portion, is composed predominantly of fibrocartilage containing only a

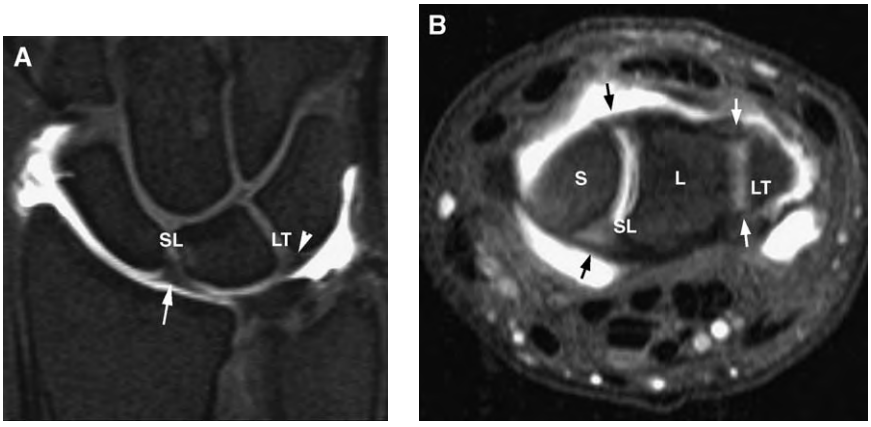

Fig. 10. Normal variations in the appearance of the scapholunate (SL) and lunotriquentral (LT) ligaments. (*A*) Coronal fat-suppressed T1-weighted MR arthrogram image showing the SL ligament with a triangular morphology (*arrow*) and a thick LT ligament with a linear morphology (*arrowhead*). (*B*) Axial fat-suppressed T1-weighted MR arthrogram image showing the dorsal and volar portions of the SL (*black arrows*) and LT ligaments (*white arrows*). L, lunate; S, scaphoid.

few superficial longitudinally-oriented collagen fibers [2,58].

Ligamentous injury

Intrinsic and extrinsic ligaments play an important role in wrist stability (Fig. 11). Injuries to the intrinsic ligaments are frequently associated with extrinsic volar and dorsal ligament lesions and often may be a cause of patients' chronic wrist pain and dysfunction. Wrist instabilities may be classified as static or dynamic [65]. Static instability refers to carpal malalignment that can be detected on standard posteroanterior and lateral radiographs, which indicate more significant and chronic ligamentous injuries [66]. Dynamic instability refers to carpal malalignment that is reproduced with physical examination maneuvers and when stress radiographs are made. With dynamic instability, there is no evidence of carpal malalignment on conventional radiographs [66].

Carpal instability is also classified into dissociative and nondissociative [59,67]. Dissociative carpal instability indicates an injury to one of the major intrinsic ligaments, such as that seen in SL dissociation and lunatotriquetral and perilunate dislocation, which may occur in association with injuries to the volar and dorsal extrinsic ligaments [66]. Nondissociative carpal instability refers to an injury to a major extrinsic ligament, with intact intrinsic ligaments, such as occurs in dorsal carpal subluxation, midcarpal instability, volar carpal subluxation, or capitate–lunate instability.

Mayfield [57] described a pattern of sequential four-stage ligamentous injury, called progressive perilunar, to be initiated on the radial aspect of the wrist and extending across the perilunate ligaments to the ulnar aspect of the wrist. Stage 1 consists of tearing the volar extrinsic radioscaphocapitate ligament with elongation or partial tearing of the SL ligament. In stage 2, with continued loading, total ligamentous failure occurs at the SL joint, followed by failure of the radioscaphocapitate ligament or an avulsion fracture of the radial styloid. Stage 3 refers to separation of the triquetrum from the lunate with associated injury to the radiolunotriquetral and dorsal radiocarpal ligament disruption. Finally, in stage 4 the ultimate failure of the dorsal radiocarpal ligament with volar lunate dislocation occurs.

Scapholunate instability

The most commonly injured ligament in the wrist is the SL [68]. SL injury usually occurs when the wrist is in hyperextension and ulnar deviation during axial compression and carpal supination. Anatomic and biomechanical testing has shown that the dorsal portion of this ligament is thicker and stronger than its volar and proximal portions [69]. It seems, however, that both the dorsal and volar components have important roles in normal SL stability. The scaphoid attachment of the SL ligament is more likely to avulse than in the stronger lunate attachment. In fact, an SL ligament tear may be associated with a scaphoid avulsion fracture.

Disruption of the SL ligament is a prerequisite for the development of SL dissociation (Fig. 12) [66]. Although isolated SL disruption does not cause an immediate and complete diastasis or abnormal radiographic alignment, biomechanical testing has shown

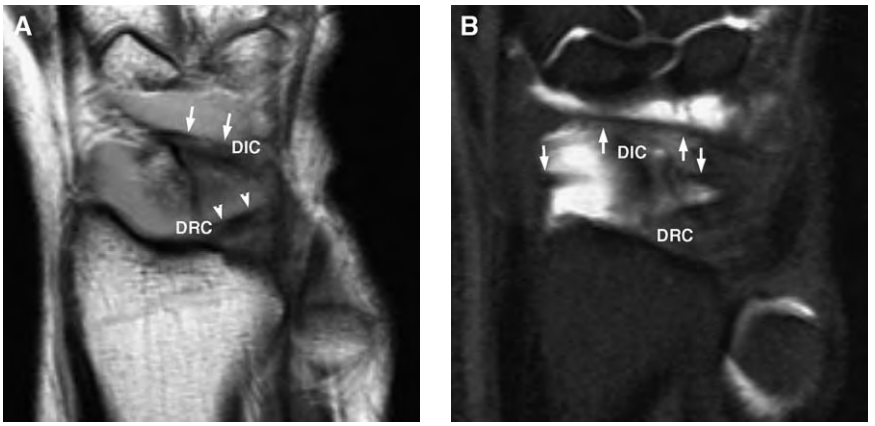

Fig. 11. Normal anatomy variants of the dorsal extrinsic ligaments. (*A*) Coronal T1-weighted MR arthrogram image showing the most common configuration of the dorsal extrinsic ligaments, the dorsal radiocarpal (DRC) ligament type I (*arrowheads*) and the dorsal intercarpal (DIC) ligament type B (*arrows*). (*B*) Coronal fat-suppressed T1-weighted MR arthrogram image showing DRC type III and DIC type C (*arrows*).

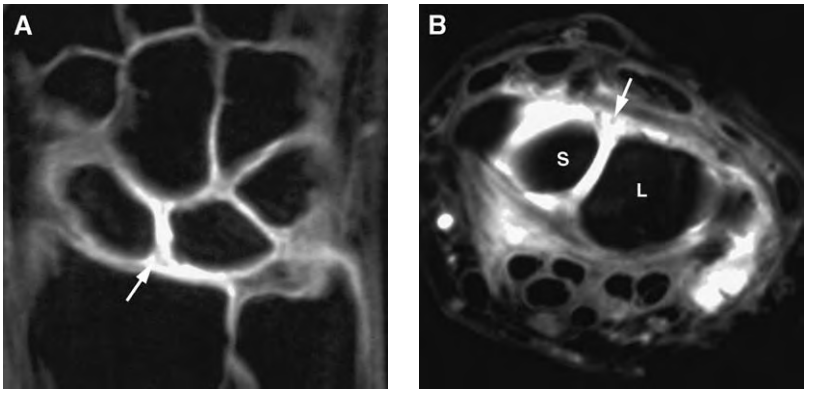

Fig. 12. Scapholunate ligament tear. (*A*) Coronal fat-suppressed T1-weighted MR arthrogram image revealing a complete SL ligament tear with a slight widening of the SL interval (*arrow*). (*B*) Axial fat-suppressed T1-weighted MR arthrogram image showing a complete tear of the dorsal component of the SL ligament (*arrow*). L, lunate; S, scaphoid.

that loss of this critical structure results in significant changes in contact load patterns and kinematics. Because the scaphoid and lunate have other strong extrinsic supporting ligaments, one or more of these ligaments must also have sustained damage to show significant radiographic changes. Presently, it is recognized that involvement of dorsal intercarpal land volar scaphotrapezial ligaments needs to occur to complete SL dissociation (Fig. 13) [62,63,70]. When left untreated, disruption of this ligament leads to progressive flexion posture of the scaphoid (rotary subluxation) and migration of the scaphoid away from the lunate. With time, a pattern of degenerative arthritis develops. Watson and Ballet [71] coined this pattern "SL advanced collapse," and postulated that it is the most common pattern of degenerative wrist arthritis. Stage I describes isolated degenerative changes between the radial styloid and distal scaphoid. Stage II describes progression of the arthrosis to the proximal scaphoid fossa and proximal scaphoid. Stage III heralds involvement of the midcarpal joint at the capitate-lunate articulation. Finally, stage IV represents the development of pancarpal degenerative arthritis.

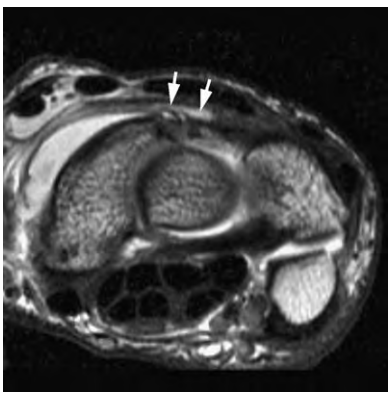

Fig. 13. Dorsal intercarpal ligament tear in a patient who has a dorsal wrist sprain. Axial T1-weighted MR arthrogram image showing thickening and fraying of the dorsal intercarpal ligament near the scaphoid attachment (*arrows*).

Patients who have SL ligament injuries experience pain with direct palpation over the SL interval. Wrist motion is only appreciably impaired after the development of carpal degenerative arthritis [66,68].

Plain radiographs are recommended in the initial evaluation of suspected SL injury. In a patient with static SL instability, a neutral posteroanterior radiograph reveals an increase in the SL interval. The clenched fist view accentuates the spacing between the scaphoid and lunate [66,68].

Instabilities involving the SL articulation may also produce a dorsal intercalated segmental instability pattern, which refers to the appearance of the lunate—the intercalated segment—on the lateral radiograph. In this pattern of instability, the lunate is dorsally angulated in the sagittal plane and the capitate is dorsally displaced toward the radiometacarpal axis (radiolunate angle, > 10° degrees). The angle formed between the longitudinal axes of the scaphoid and lunate, which normally measures 45° (±15°), is increased and greater than 70° [66,68].

MR imaging and MR arthrography. The SL ligament displays a triangular (90%) or linear morphology (10%) [23]. In 63% of cases studied by Smith [23,25], the SL ligament was seen as a homogeneous low or low-to-intermediate signal intensity structure. In 37% of cases, there were intermediate-signal

intensity areas traversing portions of the SL ligament, which can be potentially mistaken for tears.

Partial tears and elongated, but intact, ligaments may be visualized with MR imaging. A partial tear may be diagnosed when there is focal thinning or irregularity or high-signal intensity in a portion of the ligament, more commonly occurring in the central and volar portion where the weakest ligamentous attachments are located. Complete tears of the SL ligament appear as distinct areas of discontinuity within the ligament, or an absence, altogether, of the ligament. Fluid in the midcarpal joint is a sensitive, but nonspecific finding of ligament tears [20]. In more advanced cases, widening of the SL ligament articulation may be evident if complete SL ligament tears are associated with involvement of dorsal intercarpal ligament and volar scaphotrapezial ligaments [62,63,70].

MR arthrography can potentially evaluate the precise location and exact magnitude of any ligamentous defect and differentiate those lesions that may involve only the central membranous portion and be of degenerative origin [6,7]. These central lesions may be painful but not indicative of instability as would involvement of the other ligaments, particularly the dorsal portion. MR arthrography may yield an increased sensitivity to SL tears over MR imaging, especially in more subtle injuries. This includes partial tears, which may show contrast leak or imbibition into a portion of an injured ligament or better outline morphologic alterations or stretching. MR arthrography may also help outline dysfunctional ligaments that may have healed over with fibrosis or are scarred and increases the accuracy of peripheral ligament avulsions where the ligament has not lost its normal morphology. The latter may be evident clinically, but difficult to document with conventional MR imaging. In complete tears, MR arthrography shows contrast material communication between the radio- and midcarpal compartments [6,7].

The diagnostic value of MR imaging for detecting SL ligament lesions is controversial. Conventional MR imaging sensitivity ranges from 50% to 93%, specificity from 86% to 100%, and accuracy from 77% to 87% as compared with arthroscopy and surgery [6,7,20].

A recent study by Schmitt et al [8] in 125 patients suffering from wrist pain who were examined with double MR arthrography with arthroscopic correlation revealed a sensitivity of 91.7%, specificity of 100%, and accuracy of 99.2% for the detection of complete tears of the SL ligament, and a sensitivity of 62.5%, specificity of 100%, and accuracy of 95.2% for partial tears.

Treatment. Acute injuries with complete SL ligament rupture and overt dissociation should be treated as early as possible because ability of the area to heal diminishes rapidly. Often repairs are impossible after a period of 6 weeks, let alone 3 months. The ligament is usually avulsed from the scaphoid. Its reinsertion and repair is performed with transosseous stitching or mini bone anchors [72]. Nondestabilizing acute SL injuries respond to simple immobilization for 4 to 6 weeks, if minor, but require percutaneous Kirschner wiring if the injury is moderate to severe. Treatment of isolated lesions to the most proximal part of the ligament—the membranous portion—requires only arthroscopic debridement because it is mechanically inconsequential. Shaving permits immediate mobilization and rapid recovery [72].

A myriad of surgical management techniques have been performed on chronic injuries in the 1980s and 1990s, from SL arthrodesis to different ligament reconstructions [73]. Reconstruction of all structures involved (SL, dorsal intercarpal ligament, and volar scaphotrapezial ligaments) seems to be the most logical way of dealing with complete SL dissociation [74].

Lunotriquetral instability

LT injuries occur approximately one sixth as commonly as SL injuries [75,76]. Tears of the LT ligament may coexist with static and dynamic patterns of volar midcarpal instability. In patients who have volar midcarpal instability, the lunate is no longer linked to the triquetrum and follows the scaphoid. In this situation the lunate angulates palmarly (radiolunate angle, 10 degrees in a volar direction), which causes the capitate to become displaced palmar to the radiometacarpal axis. The angle formed between the longitudinal axes of the scaphoid and lunate is less than 30 degrees. An anatomic and biomechanic study performed by Viegas et al [63] found that the dorsal radiocarpal ligament must be attenuated or disrupted for a static volar midcarpal instability to develop.

Patients who have LT instability present with ulnar-sided pain. The examination of a patient who has an LT ligament tear typically reveals point tenderness over the LT interval. Plain radiographs of the wrist are usually normal in isolated LT tears. As progressive injury occurs to secondary constraints, the wrist assumes a volar midcarpal instability configuration consistent with midcarpal instability (Fig. 14) [75,76].

MR imaging and MR arthrography. The LT ligament is consistently visible with MR imaging when

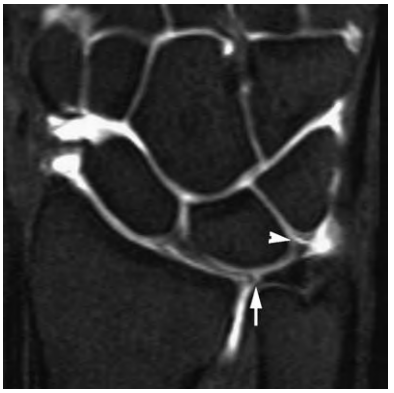

Fig. 14. Lunotriquetral ligament tear. Coronal fat-suppressed T1-weighted MR arthrogram image showing avulsion of the ulnar aspect of a delta-shaped LT ligament (*arrowhead*). Note the traumatic radial tear of the TFC (*arrow*) (Palmer class IA).

it is present. This ligament is triangular in 63% and linear in 37% of patients [24]. The signal intensity is homogeneous and low in 75%, but a brighter, linear signal traverses part or all of the LT ligament in 25% and is distinguishable from a tear because it is not quite as bright as a fluid signal.

Disruption of the ligament is shown on T2*- or fat-suppressed T2-weighted images as either complete ligamentous disruption or a discrete area of bright, linear signal intensity in a partial or complete tear. Absence of the ligament is not as useful a finding because the LT ligament may not be as reliably observed on MR imaging as the SL ligament [4,10,20,25]. Small membranous perforations may exist in the presence of intact dorsal and volar portions of the LT ligament. In fact, most degenerative perforations occur in the thin, membranous portion of the LT ligament and are difficult to appreciate on MR images. Osseous widening of the LT articulation is not usually evident even in advanced cases. Of note, the volar portion of the ligament attaches to the TFC here, which results in a discontinuous appearance—a diagnosing pitfall to be avoided.

Conventional MR imaging is less accurate in LT than SL ligament evaluation [10,11,20,22,25]. A wide range of sensitivities (40%–100%) and specificities (33%–100%) have been reported in the diagnosis of LT ligament perforations using MR imaging [4,10,20,25,26]. MR arthrography is superior to conventional MR imaging, in that it allows for identification of the size, morphology, and location of an LT ligament tear. This information is crucial because communication through a pinhole, small perforation, or deficiency in the thin membranous portion of the ligament may be insignificant in the presence of grossly intact dorsal and volar ligaments. In complete tears, contrast material communication between the radio- and midcarpal compartments may be identified [1,4,7,8].

Treatment. LT and LS ligament injury management guidelines and aftercare are similar: if diagnosed early (no later than 3 weeks after trauma) primary repair is possible and performed with transosseus reinsertion of the ligament. Chronic injuries are best currently managed through reconstruction of the ligament instead of arthrodesis, which carries a worse prognosis and high nonunion rate [77]. A tendon graft, consisting of half the extensor carpi ulnaris, is divided proximally and left distally attached, then passed through drill holes in the triquetrum and lunate, and finally sutured back to itself.

Extrinsic carpal ligaments injuries

Tears of the extrinsic volar or dorsal carpal ligaments are not commonly identified with MR imaging. Dorsal ligaments provide stability in wrist motion and are frequently injured when falling on the outstretched hand and result in a sprain of the dorsal wrist [22].

MR imaging can visualize tears of these ligaments, which appear with increased signal intensity, irregularity, and fraying, and correspond to high signal intensity on T2 sequences. MR arthrography could potentially evaluate dorsal and volar extrinsic ligaments tears because of its high resolution and excellent contrast between ligaments and surrounding structures; however, its exact use in the evaluation of these lesions is yet to be clearly defined [2,17,20,22].

Midcarpal instability

Injuries where the ligaments between the proximal carpal row bones remain intact, but the proximal and distal rows unstable is not very common [78]. This type of injury has been classified as nondissociative carpal instability [67]; an abnormality that is thought to be the result of tears, laxity, or insufficiency of the deltoid ligament ulnar limb [20,67,78]. There is also evidence of generalized ligamentous laxity. With ulnar deviation of the wrist there is a so-called "catch-up clunk" where a sudden painful snap of the proximal row occurs as the wrist is ulnarly deviated [78].

MR imaging and arthrography can visualize this kind of injury. MR arthrography allows a more precise evaluation of the ligament, although its accuracy in depicting its disruption in patients who

have clinically evident midcarpal instability has yet to be reported.

Ulnar wrist pain

Ulnar wrist pain has often been equated with low back pain because of its insidious onset, vague and chronic nature, intermittent symptoms, and the frustration that it induces in patients. Ulnar wrist pain frequently may be caused by a broad spectrum of osseous or soft tissue disorders including TFCC tears, DRUJ arthritis and instability, LT ligament disruption, Kienböck's disease, pisotriquetral arthritis, extensor carpi ulnaris lesions, and/or ulnar-sided wrist impaction syndromes [75]. The latter syndromes constitute a group of pathologic entities that result from repetitive or acute forced impaction between the distal ulna and ulnar carpus or distal radius and surrounding soft tissues and results in bone or soft tissue lesions [79,80].

In an adequate clinical setting, conventional radiographic findings of anatomic variants or pathologic conditions of the ulnar wrist can suggest the diagnosis of a given ulnar-sided impaction syndrome. Often diagnosis is difficult or delayed, however, because symptoms and clinical findings are usually nonspecific and similar among the different pathologic conditions in the ulnar-sided wrist. Moreover, significant disease and incapacitating pain may be present despite minimal evidence from conventional radiography. Conventional MR imaging and arthrography allow earlier detection of the bone and soft tissue lesions that are present in the different ulnar-sided wrist impaction syndromes [79,80].

Ulnar impaction syndrome

Ulnar impaction syndrome, also known as ulnar abutment or ulnocarpal impaction, is a degenerative condition characterized by chronic impaction between the ulnar head and the TFCC and ulnar carpus and results in a continuum of pathologic changes: TFC degenerative tear; chondromalacia of the lunate, triquetral, and distal ulnar head; LT ligament instability or tear; and, finally, osteoarthritis of the DRUJ and ulnocarpal joint.

The pathologic changes appearing in ulnar impaction syndrome most commonly occur with positive ulnar variance but can occasionally occur with neutral or negative ulnar variance [81]. The most common predisposing factors include congenital positive ulnar variance, malunion of the distal radius, premature physeal closure of the distal radius, Essex–Lopresti fracture, and previous surgical resection of the radial head. All of these predisposing factors result in a fixed increase in underlying ulnar loading associated with relative lengthening of the ulna or increased dorsal tilt of the distal radius [79,80].

In the absence of obvious structural abnormalities, ulnar impaction syndrome may result from daily activities that cause excessive intermittent loading of the ulnar carpus. It has also been shown that asymptomatic changes in ulnar impaction syndrome develop over time, so that this condition may be present even if symptoms are not evident.

The clinical manifestation of ulnar impaction syndrome generally consists of chronic or subacute ulnar wrist pain, often exacerbated by activity and relieved by rest. Pronation grip radiographs are useful in determining the increase in ulnar variance and the impaction between ulnar carpus and the dome of the ulnar head [38]. Underlying abnormalities, including malunion of a distal radial fracture with residual radial shortening and abnormal dorsal tilt, may be present. Secondary changes in the ulnar carpus include subchondral sclerosis and cystic changes in the ulnar head, ulnar aspect of the proximal lunate, and proximal radial aspect of the triquetral [82]. MR imaging and MR arthrography are helpful in detecting radiologically occult lesions [79,80,82]. Fibrillation, or partial-thickness defects of articular cartilage, in the ulnar wrist can be detected by MR arthrography; however, the accuracy of MR arthrography tends to be more favorable for high-grade or large cartilage defects [8,79,80]. Bone marrow edema can even be seen in patients who do not have cartilaginous degeneration revealed at arthroscopy, indicating that it is also a sensitive sign of ulnar impaction. Progression of the syndrome results in sclerotic changes, which appear as areas of low signal intensity on both T1- and T2-weighted images and subchondral cysts, which appear as well-defined areas of low signal intensity on T1- and high signal intensity on T2-weighted images [79,80,82].

MR arthrography may be necessary in selected cases to clarify the exact stage of ulnar impaction in the preoperative evaluation. This technique is especially useful in determining any perforation of the TFC (Palmer class IIB versus IIC) and in determining the status of the ulnocarpal ligaments and the LT ligament (Palmer class IIC versus IID) (Figs. 15 and 16).

Briefly, there are three types of procedures that can be used when dealing with symptomatic ulnar impaction: (1) the wafer procedure [48], (2) the arthroscopic wafer procedure [49], and (3) the formal ulnar shortening procedure [51]. All three aim to recede the dome of the head of the ulna. In the wafer

Fig. 15. Ulnar impaction syndrome in a patient who has LT coalition Minaar's type III and positive ulnar variance (Palmer class IIC lesion). Coronal fat-suppressed proton-density-weighted spin-echo MR arthrogram image showing degenerative central perforation of the TFC (*arrow*), chondromalacia, and subtle bone marrow edema in the ulnar aspect of the lunate bone (*arrowhead*).

procedure, the distal-most 2 to 3 mm of the dome of the ulnar head are resected by a limited approach centered on the DRUJ; this can be performed by arthroscopic instrumentation (arthroscopic wafer procedure) [48,83]. In the ulnar shortening procedure, the distal shaft of the ulna is approached dorsolaterally and the desired amount of ulna sliced away, followed by rigid fixation. Choosing which procedure to perform depends on several considerations: the amount of ulnar variance, Palmer type, shape of the sigmoid fossa and ulnar seat, presence of concomitant LT instability, and skill level of the surgeon [79,80].

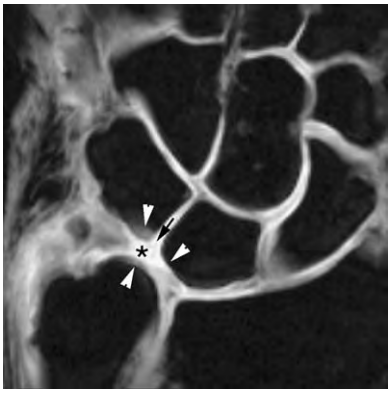

Fig. 16. Ulnar impaction syndrome (Palmer class IID lesion). Coronal fat-suppressed T1-weighted MR arthrogram image showing chondromalacia of the ulnar head, ulnar side of the lunate bone, and radial side of the triquetral bone (*arrowheads*); central perforation of the TFC (*asterisk*); and LT ligament tear (*arrow*).

Ulnar styloid impaction syndrome

Ulnar styloid impaction syndrome refers to a group of pathologic entities characterized by impaction between the ulnar styloid and the triquetrum and the surrounding soft tissues [80,84,85]. Garcia-Elias [86] has developed the ulnar styloid process index, a method that assesses the relative size of the ulnar styloid. An excessively long ulnar styloid has an ulnar styloid process index greater than 0.21 ± 0.07 or an overall length greater than 6 mm.

An elongated ulnar styloid is the most common variant implicated in the development of ulnar styloid impaction syndrome. Another anatomic variant is ulnar styloid process volarly or radially curved with a parrot-beaked appearance, which reduces significantly the styloid-carpal distance (Fig. 17) [80].

An enlarged ulnar styloid can be an anatomic variant or secondary to the malunion of the avulsion fracture at the fovea of the ulna. This ulnar styloid morphologic variation reduces the ulnar joint space causing repetitive impaction between ulnar styloid and ulnar aspect of the lunate bone and radial aspect of the triquetral [80].

Two types of ulnar styloid nonunion have been classically described anatomically and their different treatments discussed (Fig. 18) [87]. Type 1 is defined as a nonunion associated with a stable DRUJ and affects only the tip of the styloid, while the TFCC remains intact because its major attachments are at

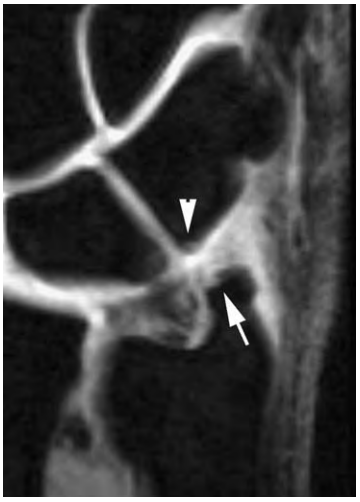

Fig. 17. Ulnar styloid impaction syndrome. Coronal fat-suppressed T1-weighted MR arthrogram image showing an excessively long ulnar styloid process, chondromalacia of the triquetral bone (*arrowhead*) and ulnar styloid tip (*arrow*), and LT ligament perforation.

Fig. 18. Ulnar styloid (US) impaction syndrome secondary to type II nonunion of the US process. Coronal fat-suppressed T1-weighted MR arthrogram image revealing nonunion of the US process (*arrow*) associated with ulnar avulsion of the TFC complex (Palmer class IB TFC complex injury) (*arrowhead*).

the base of the styloid. Type 2 is defined as a nonunion associated with DRUJ subluxation and is the result of an avulsion of the ulnar attachment of the TFCC (Palmer class IB lesion). The diagnosis of ulnar styloid impaction syndrome is based primarily on the clinical history and physical examination of the patient, and supported by radiographic evidence of morphologic variations or pathologic conditions of the ulnar styloid [80,84,85].

MR arthrography is an excellent modality for visualizing the integrity of the TFCC and its ulnar attachments, presence of nonunited bone fragments, and associated chondromalacia and subchondral bone changes of the carpus. The presence of synovitis and joint effusion in the ulnocarpal joint is also common [80].

Resection of all but the 2 proximal-most mm of the ulnar styloid (avoiding interference with TFCC insertion) is the treatment of choice in the ulnar styloid impaction syndrome secondary to elongated or parrot-beaked ulnar styloid [79,80]. Surgical treatment of the ulnar styloid impaction syndrome secondary to ulnar styloid nonunion should start with diagnostic arthroscopy that allows for classification of the condition under one of the aforementioned subtypes. If the TFCC is lax showing a positive "trampoline sign," the ulnar styloid (and with it, the TFCC) should be reinserted into the fovea and appropriately fixed by a limited incision in the ulnar aspect of the wrist. If no TFCC loosening is appreciated, the offending bony fragment should be removed [79,80].

Hamatolunate impaction syndrome

Hamatolunate impaction is a rare cause of ulnar-sided wrist pain secondary to chondromalacia of the proximal pole of the hamate bone in patients who have lunate bones with a medial articular facet on the distal surface that articulates with the hamate bone (type II lunate) [88–90]. It has been suggested that the repeated impingement and abrasion of these two bones is the mechanism that develops into chondromalacia when the wrist is in use in the full ulnar deviation position. Patients experience pain in full ulnar deviation of the wrist especially when combined with holding the distal carpal row in forced supination first.

MR arthrography may reveal defects of the articular cartilage, bone edema, sclerosis, and subchondral cysts in the proximal pole of the hamate bone [80,89]. Arthroscopic burring of the apex of the hamate represents state-of-the-art treatment of this condition [79,80].

Postoperative wrist

The increased number of patients who undergo arthroscopy and open surgical techniques to repair internal derangements of the wrist has produced an increasing demand for postoperative MR imaging evaluation because of poor outcome, recurrent symptoms, or new injury [12–14]. Several factors, however, may decrease the accuracy of MR imaging in the assessment of the postoperative wrist. These factors include surgical distortion of native anatomy, changes in signal intensity of the tissues, and image degradation caused by metallic artifacts. Radiologists should be familiar with the more common procedures currently used to repair injuries of the wrist and typical MR imaging findings in each postoperative situation to be able to recognize complications associated with such procedures [12–14].

Conventional MR imaging of postoperative TFC has unreliable results. Conventional diagnostic criteria used to diagnose TFC tears cannot be applied to postoperative TFC. Once injured, the TFC may never return to its normal, preinjury-signal intensity. Furthermore, an area of TFC healing with granulation tissue or fibrosis may appear as an abnormal signal reaching the articular surface and subject to be misinterpreted as a new tear. Additionally, TFC morphology following arthroscopy repair is abnormal, and this distortion and shape irregularity may be interpreted as a TFC tear. Specific signs of a TFC retear are a fluid-like signal within the TFC on T2-weighted images or a displaced TFC fragment [12–14]. To improve the TFC retear diagnostic accu-

racy, it is important that the preoperative images or operative reports are available for correlation with postoperative images.

MR arthrography has several advantages compared with conventional MR imaging in the evaluation of the postoperative TFC. MR arthrography uses T1-weighted images, which have a higher signal-to-noise ratio and frequently greater spatial resolution than T2-weighted images. Retears are diagnosed on MR arthrography when gadolinium signal intensity is seen extending into the TFC. In addition, increased intra-articular pressure allows for distention of normally apposed structures, such as the edges of a nondisplaced TFC tear.

MR arthrography is particularly valuable in the postoperative evaluation of symptomatic patients who have undergone reinsertion of the TFCC at the ulnaor radius (classes IB and D, respectively). TFC signal alterations extending to the TFC surface and abnormal TFC morphology can be seen at the reattachment sites on conventional MR imaging. MR arthrography with radiocarpal and DRUJ injection aids in the detection of focal TFC fillings or communicating defects in these patients, indicative of retear or inadequate reinsertion. In patients who have undergone TFC debridement or arthroscopic wafer procedure, MR arthrography is useful in identifying new TFC tears and chondral or osseous abnormalities that may occur after TFC repair (Fig. 19). MR arthrography can allow for a better evaluation of ligamentous repair techniques. MR arthrography findings become less valuable, however, when surgical reports are not available.

Ulnar collateral ligament injury

Injury to the UCL is a frequent lesion that occurs from a radially directed force on the abducted thumb [20,91,92]. This lesion was coined originally from Scottish gamekeepers who developed a chronic ligamentous strain or ‘‘gamekeeper’s thumb’’ induced by repetitive stress from the method used to kill rabbits. This type of injury is now most commonly associated with skiing and know as ‘‘skier’s thumb.’’ Rupture of the UCL may be total or partial and usually takes place at its phalangeal point of insertion, but the rupture can also appear at its metacarpal insertion or in its midsubstance. It may be accompanied by an avulsion fracture of the proximal phalanx [20,91,92]. The rupture of the thumb UCL can be an isolated lesion or occur in combination with other joint structures, such as the volar plate or dorsal capsule. When the ligament ruptures distally, retraction may be associated with the interposition of the adductor pollicis aponeurosis with the torn UCL lying superficially at the proximal end of the aponeurosis. This injury, called a Stener lesion, can inhibit proper healing of the ligament [20,91,92].

At physical examination, a complete UCL tear induces the appearance of a palpable mass in the ulnar aspect of the joint and instability to radial stress reaching an angle of 30° or higher when compared with the contralateral thumb. Nevertheless, the differentiation between a nondisplaced UCL tear and a Stener lesion may be difficult in the acute setting because of overlying soft tissue edema and hematoma [20].

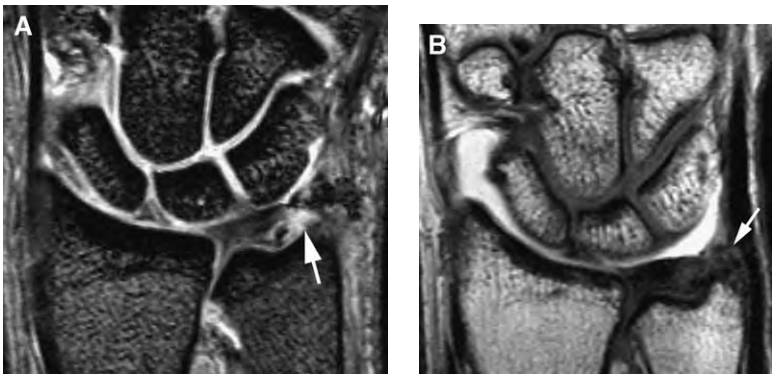

Fig. 19. Postoperative wrist. Patient who has a history of arthroscopic reinsertion of the TFC ulnar attachment (Palmer class IB lesion). (*A*) Coronal T2*-weighted conventional MR image showing persistent high-signal intensity at the TFC ulnar attachment (*arrow*) and small metallic artifacts in the ulnar aspect of the wrist. No confidence exists about the integrity of TFC ulnar attachment. (*B*) Coronal T1-weighted radiocarpal MR arthrogram image showing integrity of TFC ulnar insertion (*arrow*) with no communication between radiocarpal and DRUJ compartments.

MR imaging can detect the torn ligament and reveal displacement if present. MR imaging may also reveal any associated clinically-occult injuries involving bone or soft tissues. Primary signs of acute ligament tear include discontinuity, detachment, or thickening of the ligament associated with increased intraligamentous signal intensity on T2-weighted images. Secondary signs of acute ligament injury include soft tissue edema or hemorrhage, joint effusion, and bone bruises. MR imaging findings of a Stener lesion include UCL disruption from the base of the proximal phalanx with retraction or folding of the ligament. The ligament usually appears as a rounded or stumplike area of low-signal intensity lying superficially to the adductor aponeurosis. This characteristic MR imaging appearance has been described as a "yo-yo on a string" [20,92].

MR arthrography is more sensitive and accurate that MR imaging in the evaluation of acute and chronic UCL tears (Figs. 20 and 21) [91]. The joint distention obtained with MR arthrography allows precise assessment of the thickness of the ligament and its integrity at the insertion site. Acute or subacute tears of the UCL result in extravasation of contrast material into the adjacent soft tissues. Although MR arthrography is accurate at determining the presence of UCL ruptures and Stener lesions, the real value of MR arthrography lies in the detection of chronic ligament lesions. In this latter case, patients present with chronic pain and often joint instability. In chronic tears, secondary signs disappear and the ligament can show thickening, elongation, and an irregular or wavy contour [91].

Fig. 20. Chronic ligamentous strain of the UCL MCP joint of the thumb in a patient who has chronic pain and joint instability. Coronal fat-suppressed T1-weighted MR arthrogram image showing chronic UCL ligament thickening and tear and the irregular contour at its phalangeal point of insertion (*arrow*).

Fig. 21. Acute ligamentous strain of the UCL MCP thumb joint. Coronal fat-suppressed T1-weighted MR arthrogram image showing ligament rupture at its metacarpal insertion (*arrow*) with extravasation of contrast material into the adjacent soft tissues (*arrowhead*).

Nondisplaced UCL tears are usually treated conservatively. Surgical intervention is usually reserved for Stener lesions and complete undisplaced tears with laterolateral instability because conservative treatment leads to chronic instability and arthrosis [93,94]. Avulsion fractures involving more than 20% of the articular surface may require pinning.

Trapeziometacarpal instability

Mechanical instability of the trapeziometacarpal joint of the thumb is an important factor that may lead to articular degeneration of the joint and interfere with the normal function of the hand [95]. The anterior oblique ligament, also known as the "beak" or volar ligament, is an important joint stabilizer that limits its physiologic and radiodorsal subluxation. This ligament is a thick and broad structure that originates from the palmar tubercle of the trapezium and inserts into the beak at the base of the first metacarpal. The anterior oblique ligament is prone to rupture from a fall onto an outstretched hand where the point of contact is the base of a supinated and extended thumb metacarpal. Rupture of this ligament may cause symptomatic instability and an increased pressure on the incongruous articular cartilage, which may lead to osteoarthritis [95].

MR arthrography is useful in the detection of acute or chronic ruptures of the anterior oblique ligament. In acute ruptures, MR arthrography reveals stretching or discontinuity of the ligament with contrast extravasation. The most frequent findings in chronic rupture are elongation, thickening, and an irregular and wavy contour (Fig. 22).

Fig. 22. Trapeziometacarpal instability. Coronal T1-weighted MR arthrogram image revealing a chronic rupture of the anterior oblique ligament with elongation, thickening, and a wavy contour of the ligament (*arrow*).

In most patients conservative treatment gives good results. Patients who have symptomatic instability may require reconstruction of the ligament to avoid any compromise to the function of the thumb [95].

Metacarpophalangeal lesions of the fingers

Collateral ligament injuries in the metacarpophalangeal joints of the fingers are rare compared with those of the thumb. Almost all collateral ligament tears in the fingers occur on the radial side [96,97]. The most commonly involved digit is the index finger, followed by the little finger. On the ulnar side of the little finger, displacement of the torn ligament over the intact sagittal band of the extensor hood may occur, similar to the Stener lesion of the first metacarpophalangeal joint. The displacement of the torn ligament interferes with healing and necessitates surgery [97].

MR arthrography can be used in the evaluation of selected cases of collateral ligament tears (ligamentous tears with articular instability) and volar plate lesions of the metacarpophalangeal joints. MR arthrography imaging criteria for diagnosis of acute collateral ligament tears include discontinuity, detachment, or thickening of the ligament. Extravasation of contrast solution into the adjacent soft tissues may also be observed in acute or subacute settings. Chronic tears often show thickening of the ligament, which is probably secondary to scar formation. Elongation, or a wavy ligament contour ligament, may also be seen. Injuries of the volar plate can be seen in MR arthrography as a disrupted attachment with a gap and ventral extravasation of contrast where avulsion of the volar plate takes place.

Although most lesions are treated conservatively, surgery has been advocated in cases of severe metacarpophalangeal instability or intra-articular displacement of the torn ligament [97].

Indirect MR arthrography

Indirect MR arthrography is based on the premise that intravenous administration of gadolinium followed by 5 to 10 minutes of light exercise leads to an enhancement effect in joints [98–100]. Indirect MR arthrography has been developed as an alternative, less invasive imaging technique than direct MR arthrography for joint assessment. Homogeneous enhancement of joint structures can be achieved with indirect MR arthrography, but it lacks controlled capsular distention. Some authors have reported good initial results with this technique in the evaluation of the TFCC and intrinsic ligaments of the wrist; however, a recent study concluded that although indirect MR arthrography improves sensitivity in the evaluation of the SL ligament when compared with conventional MR imaging, it does not significantly improve the ability to evaluate the TFCC or the LT ligament [99]. The major advantage of indirect arthrography of the wrist lies in detection of abnormalities other than the usual internal derangements. With indirect MR arthrography there is enhancement of fluid within the tendon sheath in the presence of tenosynovitis. Enhancement around flexor tendons even without increased fluid is a relatively specific sign of carpal tunnel syndrome. Subtle cartilage defects can be identified by associated subchondral enhancement [98].

Summary

Radiocarpal MR arthrography is an excellent technique for determining the localization, size, and extent of pathologic lesions of the TFCC and the intrinsic ligaments of the proximal row of the wrist. Triple-compartment MR arthrography is useful in the evaluation of patients who have refractory pain or instability syndromes of the wrist. Other evolving applications of MR arthrography of the wrist are ulnar-sided impaction syndromes and postoperative evaluation of TFCC and ligaments.

MR arthrography also may be applied in the diagnosis of selected pathologies of the small joints

of the hand, such as UCL tears of the metacarpophalangeal of the thumb, tears of the anterior-oblique ligament of the trapeziometacarpal joint, and lesions of the collateral ligaments and volar plate tears of the metacarpophalangeal joints of the fingers. MR arthrography cannot replace wrist arthroscopy; however, it can facilitate the diagnosis and the indication for surgery and reduce the number of diagnostic arthroscopic interventions.

References

[1] Braun H, Kenn W, Schneider S, et al. Direct MR arthrography of the wrist: value in detecting complete and partial defects of intrinsic ligaments and the TFCC in comparison with arthroscopy. Rofo Fortschr Geb Rontgenstr Neuen Bildgeb Verfahr 2003;175: 1515–24.

[2] Brown RR, Fliszar E, Cotten A, et al. Extrinsic and intrinsic ligaments of the wrist: normal and pathologic anatomy at MR arthrography with three-compartment enhancement. Radiographics 1998;18:667–74.

[3] Carrino JA, Smith DK, Schweitzer ME. MR arthrography of the elbow and wrist. Semin Musculoskelet Radiol 1998;2:397–414.

[4] Kovanlikaya I, Camli D, Cakmakci H, et al. Diagnostic value of MR arthrography in detection of intrinsic carpal ligament lesions: use of cine-MR arthrography as a new approach. Eur Radiol 1997;7: 1441–5.

[5] Palmer WE. MR arthrography: is it worthwhile? Top Magn Reson Imaging 1996;8:24–43.

[6] Scheck RJ, Kubitzek C, Hierner R, et al. The scapholunate interosseous ligament in MR arthrography of the wrist: correlation with non-enhanced MRI and wrist arthroscopy. Skeletal Radiol 1997;26: 263–71.

[7] Scheck RJ, Romagnolo A, Hierner R, et al. The carpal ligaments in MR arthrography of the wrist: correlation with standard MRI and wrist arthroscopy. J Magn Reson Imaging 1999;9:468–74.

[8] Schmitt R, Christopoulos G, Meier R, et al. Direct MR arthrography of the wrist in comparison with arthroscopy: a prospective study on 125 patients. Rofo Fortschr Geb Rontgenstr Neuen Bildgeb Verfahr 2003;175:911–9.

[9] Schulte-Altedorneburg G, Gebhard M, Wohlgemuth WA, et al. MR arthrography: pharmacology, efficacy and safety in clinical trials. Skeletal Radiol 2003;32: 1–12.

[10] Schweitzer ME, Brahme SK, Hodler J, et al. Chronic wrist pain: spin-echo and short tau inversion recovery MR imaging and conventional and MR arthrography. Radiology 1992;182:205–11.

[11] Zanetti M, Bram J, Hodler J. Triangular fibrocartilage and intercarpal ligaments of the wrist: does MR arthrography improve standard MRI? J Magn Reson Imaging 1997;7:590–4.

[12] Grainger AJ, Elliott JM, Campbell RS, et al. Direct MR arthrography: a review of current use. Clin Radiol 2000;55:163–76.

[13] Peh WC, Cassar-Pullicino VN. Magnetic resonance arthrography: current status. Clin Radiol 1999;54: 575–87.

[14] Steinbach LS, Palmer WE, Schweitzer ME. Special focus session: MR arthrography. Radiographics 2002; 22:1223–46.

[15] Linkous MD, Gilula LA. Wrist arthrography today. Radiol Clin North Am 1998;36:651–72.

[16] Brown RR, Clarke DW, Daffner RH. Is a mixture of gadolinium and iodinated contrast material safe during MR arthrography? AJR Am J Roentgenol 2000;175:1087–90.

[17] Theumann NH, Pfirrmann CW, Antonio GE, et al. Extrinsic carpal ligaments: normal MR arthrographic appearance in cadavers. Radiology 2003;226:171–9.

[18] Beaulieu CF, Ladd AL. MR arthrography of the wrist: scanning-room injection of the radiocarpal joint based on clinical landmarks. AJR Am J Roentgenol 1998; 170:606–8.

[19] Yoshioka H, Ueno T, Tanaka T, et al. High-resolution MR imaging of triangular fibrocartilage complex (TFCC): comparison of microscopy coils and a conventional small surface coil. Skeletal Radiol 2003; 32:575–81.

[20] Zlatkin MB, Rosner J. MR imaging of ligaments and triangular fibrocartilage complex of the wrist. Magn Reson Imaging Clin N Am 2004;12:301–31.

[21] Yu JS, Habib PA. Normal MR imaging anatomy of the wrist and hand. Magn Reson Imaging Clin N Am 2004;12:207–19.

[22] Stoller D, Brody G. The wrist and hand. In: Stoller D, editor. Magnetic resonance imaging in orthopaedics and sports medicine. Philadelphia: Lippincott-Raven Publishers; 1997. p. 851–993.

[23] Smith DK. Scapholunate interosseous ligament of the wrist: MR appearances in asymptomatic volunteers and arthrographically normal wrists. Radiology 1994; 192:217–21.

[24] Smith DK, Snearly WN. Lunotriquetral interosseous ligament of the wrist: MR appearances in asymptomatic volunteers and arthrographically normal wrists. Radiology 1994;191:199–202.

[25] Smith DK. MR imaging of normal and injured wrist ligaments. Magn Reson Imaging Clin N Am 1995;3: 229–48.

[26] Totterman SM, Miller R, Wasserman B, et al. Intrinsic and extrinsic carpal ligaments: evaluation by three-dimensional Fourier transform MR imaging. AJR Am J Roentgenol 1993;160:117–23.

[27] Totterman SM, Miller RJ. MR imaging of the triangular fibrocartilage complex. Magn Reson Imaging Clin N Am 1995;3:213–28.

[28] Totterman SM, Miller RJ, McCance SE, et al. Lesions of the triangular fibrocartilage complex: MR findings

with a three-dimensional gradient-recalled-echo sequence. Radiology 1996;199:227–32.
[29] Palmer AK, Werner FW. The triangular fibrocartilage complex of the wrist: anatomy and function. J Hand Surg 1981;6:153–62.
[30] Garcia-Elias M. Soft-tissue anatomy and relationships about the distal ulna. Hand Clin 1998;14:165–76.
[31] Thiru RG, Ferlic DC, Clayton ML, et al. Arterial anatomy of the triangular fibrocartilage of the wrist and its surgical significance. J Hand Surg [Am] 1986; 11:258–63.
[32] Benjamin M, Evans EJ, Pemberton DJ. Histological studies on the triangular fibrocartilage complex of the wrist. J Anat 1990;172:59–67.
[33] Chidgey LK, Dell PC, Bittar ES, et al. Histologic anatomy of the triangular fibrocartilage. J Hand Surg [Am] 1991;16:1084–100.
[34] Mikic ZD. Age changes in the triangular fibrocartilage of the wrist joint. J Anat 1978;126:367–84.
[35] Cooney WP, Linscheid RL, Dobyns JH. Triangular fibrocartilage tears. J Hand Surg [Am] 1994;19: 143–54.
[36] Dailey SW, Palmer AK. The role of arthroscopy in the evaluation and treatment of triangular fibrocartilage complex injuries in athletes. Hand Clin 2000;16: 461–76.
[37] Palmer AK. Triangular fibrocartilage complex lesions: a classification. J Hand Surg 1989;14:594–606.
[38] Friedman SL, Palmer AK. The ulnar impaction syndrome. Hand Clin 1991;7:295–310.
[39] Gilula LA, Palmer AK. Is it possible to call a "tear" on arthrograms or magnetic resonance imaging scans? J Hand Surg [Am] 1993;18:547.
[40] Zanetti M, Linkous MD, Gilula LA, et al. Characteristics of triangular fibrocartilage defects in symptomatic and contralateral asymptomatic wrists. Radiology 2000;216:840–5.
[41] Haims AH, Schweitzer ME, Morrison WB, et al. Limitations of MR imaging in the diagnosis of peripheral tears of the triangular fibrocartilage of the wrist. AJR Am J Roentgenol 2002;178:419–22.
[42] Morley J, Bidwell J, Bransby-Zachary M. A comparison of the findings of wrist arthroscopy and magnetic resonance imaging in the investigation of wrist pain. J Hand Surg 2001;26:544–6.
[43] Oneson SR, Scales LM, Erickson SJ, et al. MR imaging of the painful wrist. Radiographics 1996;16: 997–1008.
[44] Oneson SR, Timins ME, Scales LM, et al. MR imaging diagnosis of triangular fibrocartilage pathology with arthroscopic correlation. AJR Am J Roentgenol 1997;168:1513–8.
[45] Potter HG, Asnis-Ernberg L, Weiland AJ, et al. The utility of high-resolution magnetic resonance imaging in the evaluation of the triangular fibrocartilage complex of the wrist. J Bone Joint Surg Am 1997;79: 1675–84.
[46] Bernstein MA, Nagle DJ, Martinez A, et al. A comparison of combined arthroscopic triangular fibrocartilage complex debridement and arthroscopic wafer distal ulna resection versus arthroscopic triangular fibrocartilage complex debridement and ulnar shortening osteotomy for ulnocarpal abutment syndrome. Arthroscopy 2004;20:392–401.
[47] Geissler WB, Freeland AE, Weiss AP, et al. Techniques of wrist arthroscopy. Instr Course Lect 2000; 49:225–37.
[48] Feldon P, Terrono AL, Belsky MR. The "wafer" procedure: partial distal ulnar resection. Clin Orthop 1992;275:124–9.
[49] Loftus JB. Arthroscopic wafer for ulnar impaction syndrome. Tech Hand Upper Extrem Surg 2000;4: 182–8.
[50] Hermansdorfer JD, Kleinman WB. Management of chronic peripheral tears of the triangular fibrocartilage complex. J Hand Surg 1991;16:340–6.
[51] Minami A, Kato H. Ulnar shortening for triangular fibrocartilage complex tears associated with ulnar positive variance. J Hand Surg [Am] 1998;23:904–8.
[52] Trumble TE, Gilbert M, Vedder N. Ulnar shortening combined with arthroscopic repairs in the delayed management of triangular fibrocartilage complex tears. J Hand Surg [Am] 1997;22:807–13.
[53] Melone Jr CP, Nathan R. Traumatic disruption of the triangular fibrocartilage complex. Pathoanatomy. Clin Orthop 1992;275:65–73.
[54] Scheker LR, Belliappa PP, Acosta R, et al. Reconstruction of the dorsal ligament of the triangular fibrocartilage complex. J Hand Surg 1994;19:310–8.
[55] Jantea CL, Baltzer A, Ruther W. Arthroscopic repair of radial-sided lesions of the triangular fibrocartilage complex. Hand Clin 1995;11:31–6.
[56] Taleisnik J. The ligaments of the wrist. J Hand Surg [Am] 1976;1:110–8.
[57] Mayfield JK. Wrist ligamentous anatomy and pathogenesis of carpal instability. Orthop Clin North Am 1984;15:209–16.
[58] Berger RA. The anatomy of the ligaments of the wrist and distal radioulnar joints. Clin Orthop 2001;383: 32–40.
[59] Cooney WP, Dobyns JH, Linscheid RL. Arthroscopy of the wrist: anatomy and classification of carpal instability. Arthroscopy 1990;6:133–40.
[60] Timins ME, Jahnke JP, Krah SF, et al. MR imaging of the major carpal stabilizing ligaments: normal anatomy and clinical examples. Radiographics 1995;15: 575–87.
[61] Mitsuyasu H, Patterson RM, Shah MA, et al. The role of the dorsal intercarpal ligament in dynamic and static scapholunate instability. J Hand Surg [Am] 2004;29:279–88.
[62] Mizuseki T, Ikuta Y. The dorsal carpal ligaments: their anatomy and function. J Hand Surg 1989;14:91–8.
[63] Viegas SF, Yamaguchi S, Boyd NL, et al. The dorsal ligaments of the wrist: anatomy, mechanical properties, and function. J Hand Surg [Am] 1999;24:456–68.
[64] Berger RA, Kauer JM, Landsmeer JM. Radioscapholunate ligament: a gross anatomic and histologic

study of fetal and adult wrists. J Hand Surg [Am] 1991;16:350–5.
[65] Linscheid RL, Dobyns JH, Beabout JW, et al. Traumatic instability of the wrist: diagnosis, classification, and pathomechanics. J Bone Joint Surg Am 1972;54:1612–32.
[66] Gelberman RH, Cooney III WP, Szabo RM. Carpal instability. Instr Course Lect 2001;50:123–34.
[67] Wright TW, Dobyns JH, Linscheid RL, et al. Carpal instability non-dissociative. J Hand Surg 1994;19: 763–73.
[68] Shin SS, Moore DC, McGovern RD, et al. Scapholunate ligament reconstruction using a bone-retinaculum-bone autograft: a biomechanic and histologic study. J Hand Surg [Am] 1998;23:216–21.
[69] Linkous MD, Pierce SD, Gilula LA. Scapholunate ligamentous communicating defects in symptomatic and asymptomatic wrists: characteristics. Radiology 2000;216:846–50.
[70] Moritomo H, Viegas SF, Elder K, et al. The scaphotrapezio-trapezoidal joint. Part 2: A kinematic study. J Hand Surg [Am] 2000;25:911–20.
[71] Watson HK, Ballet FL. The SLAC wrist: scapholunate advanced collapse pattern of degenerative arthritis. J Hand Surg [Am] 1984;9:358–65.
[72] Adolfsson L. Arthroscopic diagnosis of ligament lesions of the wrist. J Hand Surg 1994;19:505–12.
[73] Blatt G. Capsulodesis in reconstructive hand surgery: dorsal capsulodesis for the unstable scaphoid and volar capsulodesis following excision of the distal ulna. Hand Clin 1987;3:81–102.
[74] Walsh JJ, Berger RA, Cooney WP. Current status of scapholunate interosseous ligament injuries. J Am Acad Orthop Surg 2002;10:32–42.
[75] Shin A, Deitch M, Sachar K, et al. Ulnar-sided wrist pain: diagnosis and treatment. J Bone Joint Surg Am 2004;86A:1560–74.
[76] Weiss LE, Taras JS, Sweet S, et al. Lunotriquetral injuries in the athlete. Hand Clin 2000;16:433–8.
[77] Shin AY, Weinstein LP, Berger RA, et al. Treatment of isolated injuries of the lunotriquetral ligament: a comparison of arthrodesis, ligament reconstruction and ligament repair. J Bone Joint Surg Br 2001;83: 1023–8.
[78] Brown DE, Lichtman DM. Midcarpal instability. Hand Clin 1987;3:135–40.
[79] Cerezal L, del Pinal F, Abascal F, et al. Imaging findings in ulnar-sided wrist impaction syndromes. Radiographics 2002;22:105–21.
[80] Cerezal L, del Pinal F, Abascal F. MR imaging findings in ulnar-sided wrist impaction syndromes. Magn Reson Imaging Clin N Am 2004;12:281–99.
[81] Tomaino MM. Ulnar impaction syndrome in the ulnar negative and neutral wrist: diagnosis and pathoanatomy. J Hand Surg 1998;23:754–7.
[82] Imaeda T, Nakamura R, Shionoya K, et al. Ulnar impaction syndrome: MR imaging findings. Radiology 1996;201:495–500.
[83] Tomaino MM, Weiser RW. Combined arthroscopic TFCC debridement and wafer resection of the distal ulna in wrists with triangular fibrocartilage complex tears and positive ulnar variance. J Hand Surg [Am] 2001;26:1047–52.
[84] Tomaino MM, Gainer M, Towers JD. Carpal impaction with the ulnar styloid process: treatment with partial styloid resection. J Hand Surg 2001;26:252–5.
[85] Topper SM, Wood MB, Ruby LK. Ulnar styloid impaction syndrome. J Hand Surg 1997;22:699–704.
[86] Garcia-Elias M. Dorsal fractures of the triquetrum-avulsion or compression fractures? J Hand Surg 1987; 12:266–8.
[87] Hauck RM, Skahen III J, Palmer AK. Classification and treatment of ulnar styloid nonunion. J Hand Surg 1996;21:418–22.
[88] Malik AM, Schweitzer ME, Culp RW, et al. MR imaging of the type II lunate bone: frequency, extent, and associated findings. AJR Am J Roentgenol 1999; 173:335–8.
[89] Pfirrmann CW, Theumann NH, Chung CB, et al. The hamatolunate facet: characterization and association with cartilage lesions: magnetic resonance arthrography and anatomic correlation in cadaveric wrists. Skeletal Radiol 2002;31:451–6.
[90] Thurston AJ, Stanley JK. Hamato-lunate impingement: an uncommon cause of ulnar-sided wrist pain. Arthroscopy 2000;16:540–4.
[91] Harper MT, Chandnani VP, Spaeth J, et al. Gamekeeper thumb: diagnosis of ulnar collateral ligament injury using magnetic resonance imaging, magnetic resonance arthrography and stress radiography. J Magn Reson Imaging 1996;6:322–8.
[92] Plancher KD, Ho CP, Cofield SS, et al. Role of MR imaging in the management of "skier's thumb" injuries. Magn Reson Imaging Clin N Am 1999;7:73–84.
[93] Melone Jr CP, Beldner S, Basuk RS. Thumb collateral ligament injuries: an anatomic basis for treatment. Hand Clin 2000;16:345–57.
[94] Fairhurst M, Hansen L. Treatment of "gamekeeper's thumb" by reconstruction of the ulnar collateral ligament. J Hand Surg 2002;27:542–5.
[95] Barron OA, Glickel SZ, Eaton RG. Basal joint arthritis of the thumb. J Am Acad Orthop Surg 2000;8: 314–23.
[96] Masson JA, Golimbu CN, Grossman JA. MR imaging of the metacarpophalangeal joints. Magn Reson Imaging Clin N Am 1995;3:313–25.
[97] Pomerance JF. Painful basal joint arthritis of the thumb. Part II: Treatment. Am J Orthop 1995;24: 466–72.
[98] Bergin D, Schweitzer ME. Indirect magnetic resonance arthrography. Skeletal Radiol 2003;32:551–8.
[99] Haims AH, Schweitzer ME, Morrison WB, et al. Internal derangement of the wrist: indirect MR arthrography versus unenhanced MR imaging. Radiology 2003;227:701–7.
[100] Vahlensieck M, Peterfy CG, Wischer T, et al. Indirect MR arthrography: optimization and clinical applications. Radiology 1996;200:249–54.